# Electric Strength of Epoxide Resins and Its Relation to the Structure

TAKASHI TAKAHAMA, OSAMU HAYASHI, and FUMIHIKO SATO,
*Manufacturing Development Laboratory, Mitsubishi Electric Corporation Minamishimizu, Amagasaki, Hyogo, Japan*

## Synopsis

Epoxide resins having various ratios of ether and ester bonds were investigated as to the relation between electric strength and polymer characteristics. The electric strength over a wide range of temperature is presented here. A marked reduction of strength characteristics of the epoxide resins occurs at a critical temperature indistinguishable from the glass transition temperature $T_g$, which is related to the free volume and molecular relaxation process. At temperatures exceeding $T_g$, the electric strength has a strong dependence on polymer structure, film thickness, and applied pulse width. This behavior is considered to obey the thermal breakdown mechanism, and it is assumed that the ion is important in the precursory region of electric breakdown.

## INTRODUCTION

Epoxide resins have attracted considerable attention as electrical insulating material because of excellent electrical properties as well as a variety of other physical, chemical, and mechanical properties.[1] However, the factors and relations which determine the electric strength of epoxide resins are little known since the complicated structure of cured epoxide resins[2] prevents the mechanism of electric breakdown with respect to the structures from being revealed. Milton[3] observed that the strength of epoxide resins varies from about 0.8 to near 3.2 mV/cm, depending on the curing temperature and casting mold materials. Cuthrell[4–6] also pointed out the importance of residual liquid constituents of epoxide resins for electric breakdown. In this report, epoxide resins cured as completely as possible and having various ratios of ether and ester bonds were selected with a view to correlating the results with structure. The behavior of the abrupt changes in electric strength of polymers as a function of temperature is presented, and the mechanism of electric breakdown and its relations to structures is discussed.

## EXPERIMENTAL

### Materials

Epoxide resin films were prepared from purified diglycidyl ether of bisphenol A (Shell Chem. Co.), and different amounts of methyltetrahydrophthalic acid anhydride curing agent with 2-ethyl-4-methylimidazole as accelerator were added as listed in Table I. To investigate the electrical properties of epoxide resins, films 30–200 $\mu$m thick were cast on Teflon film-coated glass plates. The resin and hardener were outgassed and heated at 150°C for 15 hr, then postcured at 200°C for 4 hr.

Journal of Applied Polymer Science, Vol. 26, 2211–2220 (1981)
 CCC 0021-8995/80/072211-10$01.00

TABLE I
Composition

| Sample No. | Acid anhydride[a]/ epoxy resin,[b] equiv | Remarks |
|---|---|---|
| 1 | 0 | catalyst: |
| 2 | 0.5 | 2E4M imidazole |
| 3 | 1.0 | 3 phr |

[a] Methyltetrahydrophthalic acid anhydride.
[b] Bisphenol-type epoxy resin (Epikote 828).

## Measurements

Specific volume was measured by the change of sample weight in silicon oil, which was used as ambient medium.

Dynamic mechanical properties were measured with a free oscillating torsion pendulum (approximately 1 Hz in frequency) between room temperature and 200°C.

Electric strength measurements were carried out by a Cockcroft-type dc generator and an electron tube-type pulse generator. A test film thickness of 50 ± 10 $\mu$m was typically chosen, except for the film thickness dependence measurements. The film was held by light pressure between sphere/plane electrodes shown in Figure 1, and silicon fluid was used as an immersion medium. Values of electric strength that were extremely low in comparison with other values obtained under the same condition were discarded, and plots of the electric strength on a total of more than ten specimens represent the mean of the number of samples designated at each point; the vertical lines indicate the corresponding standard deviations.

Electrical conductivity measurements as a function of temperature were carried out in dry nitrogen gas with a vibration-reed electrometer (Keithley Co.). Films were set at 240°C in a 5 kV/cm dc field to remove the absorption current completely; thereafter the steady-state current was measured for temperature decrease.

Current density measurements from low to high electric fields were carried out at 150°C, and the current value 1 min after voltage application was adopted.

Dielectric properties were measured by an ac bridge at a single measurement frequency of 60 Hz from room temperature to 190°C.

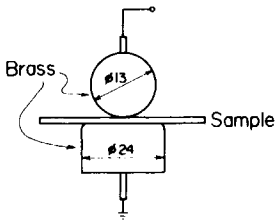


Fig. 1. Form of the electrodes.

## RESULTS

### Characteristics of Materials

The structure of cured epoxide resins is complicated, but if the reaction between the epoxy group and the acid anhydride occurs completely and the rest of the epoxy groups react mutually, various ratios of ether and ester bonds could be determined by controlling the amount of acid anhydride. Figure 2 shows structural schemes of epoxide resin network based on ester and ether bond, respectively.

The temperature dependence of the specific volume is shown in Figure 3. The intersections of the oblique lines correspond to the glass transition temperatures $T_g$ of the samples. Introduction of an ester link into epoxide resin networks causes a higher $T_g$ temperature and reduces the specific volume.

Figure 4 shows the dynamic mechanical properties of these samples. Introduction of an ester link into the epoxide resins decreases the modulus of the rubbery state region and increases the temperature of the tan $\delta$ peak. Above

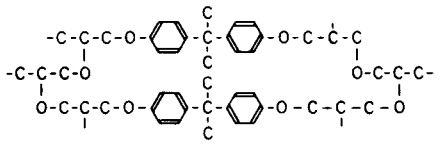

Etherbond (Sample 1)

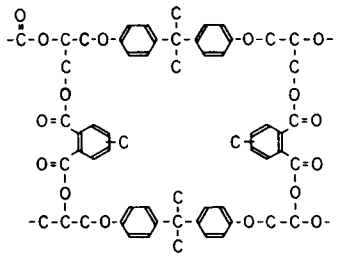

Esterbond (Sample 3)

Fig. 2. Structural schemes of epoxide resin network.

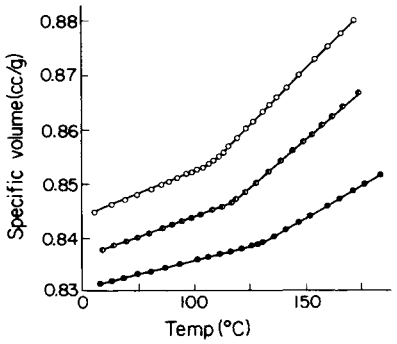


Fig. 3. Specific volume vs. temperature for epoxide resins: (○) sample 1; (◐) sample 2; (●) sample 3.

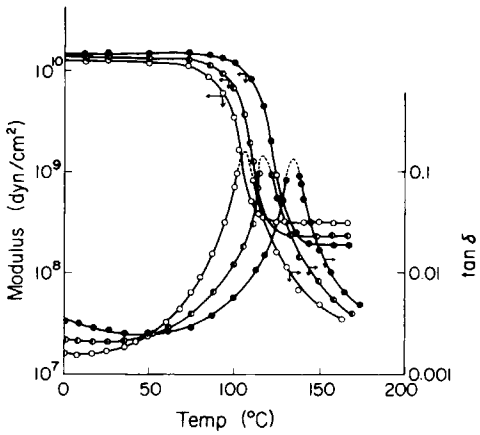


Fig. 4. Dynamic mechanical properties of epoxide resins: (○) sample 1; (◐) sample 2; (●) sample 3.

$T_g$, the epoxide resins are highly crosslinked elastomers; in principle the crosslink density $\rho$ can be obtained from dynamic mechanical data using the theory of rubberlike elasticity given by[7]

$$\rho_R = \phi \frac{\upsilon E'_2}{3RT} \tag{1}$$

where $\rho_R$ is the crosslink density, $\phi$ the front factor, $\upsilon$ the specific volume, $R$ the gas constant, $T$ the absolute temperature, and $E'_2$ the equilibrium modulus. It is also possible to obtain the crosslink density $\rho_s$ from the stoichiometrical equivalent ratio of the components calculated on the assumption that the tetrafunctional backbone chain which is obtained from the reaction of 1 mole epoxide resin with either 0, 1, or 2 moles anhydride acid forms a regularly arranged cubic network of freely jointed chains.[8,9] Values of characteristic parameters representing $\rho_R$ and $\rho_S$ are given in Table II, where $\phi$ is 1 for each sample. The good coincidence of $\rho_R$ and $\rho_S$ shows that these epoxide resins have been cured as expected. Evidence of complete cure may be also obtained from an infrared spectrum. The absorption band occurring at 10.95 $\mu$m is associated with a polymer epoxy group. The sample polymers exhibit little absorption at this wavelength, and this qualitatively confirms complete cure.

TABLE II
Characteristics Parameter Representing Crosslink Density $\rho_R$ and Comparison of $\rho_R$ and $\rho_S$[a]

| Sample No. | $T$, °C | $E'_2 \times 10^{-8}$, dyn/cm² | $\upsilon$, cc/g | $\rho_R \times 10^3$, moles/g | $\rho_S \times 10^3$, moles/g |
|---|---|---|---|---|---|
| 1 | 108 | 3.3 | 0.895 | 2.6 | 2.6 |
| 2 | 115 | 2.1 | 0.884 | 2.0 | 1.8 |
| 3 | 125 | 1.8 | 0.865 | 1.6 | 1.4 |

[a] $E'_2$, Equilibrium dynamic modulus at $T_g$ + 80°C; $\upsilon$, specific volume at Tg + 80°C; $\rho_R$, crosslink density calculated by eq. (1); $\rho_S$, crosslink density calculated from the concentration of components.

## Electrical Properties

Electric strength results for the epoxide resins examined by applying dc voltage are shown in Figure 5. The strength is constant up to more than 100°C and decreases rapidly with further temperature increase. In the high-temperature region, sample 1 shows a higher electric strength than sample 3, with sample 2 in the middle. These results strongly reflect the structural features, and the introduction of ester links causes the electric strength to decrease. Figure 6 clearly shows the electric strength around the critical temperature indicated in Figure 5, at which a marked reduction of the strength occurs. Different critical temperatures are observed in each sample; introduction of an ester link also causes this temperature to increase.

Figure 7 shows the dependence of electric strength on sample thickness at 150°C. The strength of both samples with ester link and ether link, respectively, shows the same dependence of film thickness and the strength decrease in accordance with the increase in film thickness. Figure 8 shows the measured electric strength in sample 1 as a temperature function by applying a dc pulse voltage with different pulse width, and Figure 9 shows the measured electric strength in sample 3. Both these data show that the strength is constant up to near 100°C, conforming the results shown in Figure 5. It is however in the

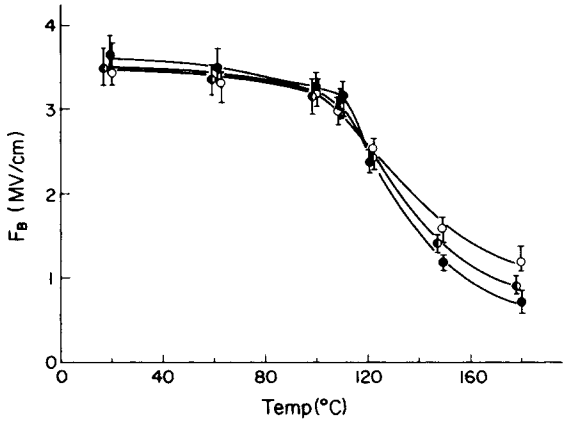


Fig. 5. Electric strength ($F_B$) vs. temperature for epoxide resins with applied dc voltage: (○) sample 1; (◐) sample 2; (●) sample 3.

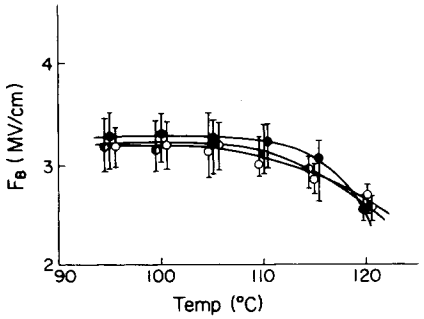


Fig. 6. Electric strength ($F_B$) of critical temperature region for epoxide resins with applied d.c. voltage: (○) sample 1; (◐) sample 2; (●) sample 3.

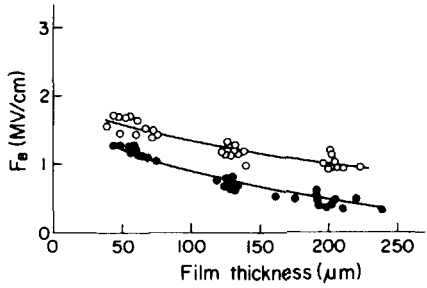


Fig. 7. Electric strength ($F_B$) vs. film thickness for epoxide resins with applied dc voltage at 150°C: (○) sample 1; (●) sample 3.

high-temperature region that the strength decrease depends on the pulse width. Increasing the temperature and pulse width decreases the strength markedly, and in sample 3 this tendency is enhanced compared with sample 1.

Temperature dependence of electrical conductivity is shown in Figure 10. The conductivity increases abruptly in the $T_g$ region and gives a large activation energy above this temperature. The general features of the dielectric loss peak for epoxide resins are illustrated at 60 Hz as a function of temperature in Figure 11. The loss peaks for these samples reflect $\alpha$-relaxation; virtually identical behavior was observed in terms of the magnitude and temperature location of the dielectric loss peak.

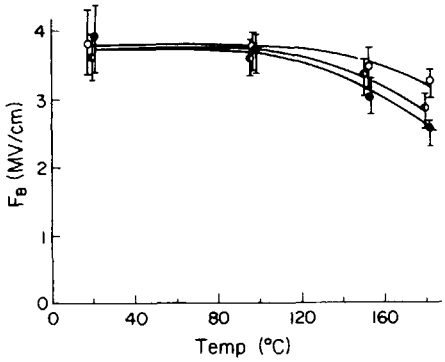


Fig. 8. Electric strength ($F_B$) vs. temperature on pulse width for sample 1.

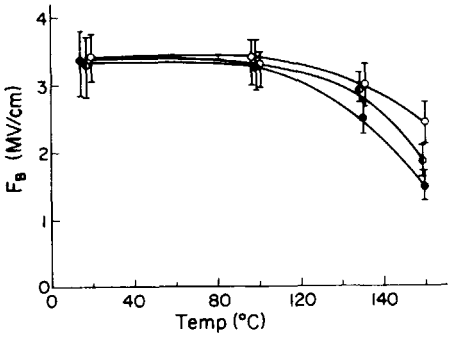


Fig. 9. Electric strength ($F_B$) vs. temperature on pulse width for sample 3. Pulse width (μsec): (○) $10^1$; (◐) $10^2$; (●) $10^3$.

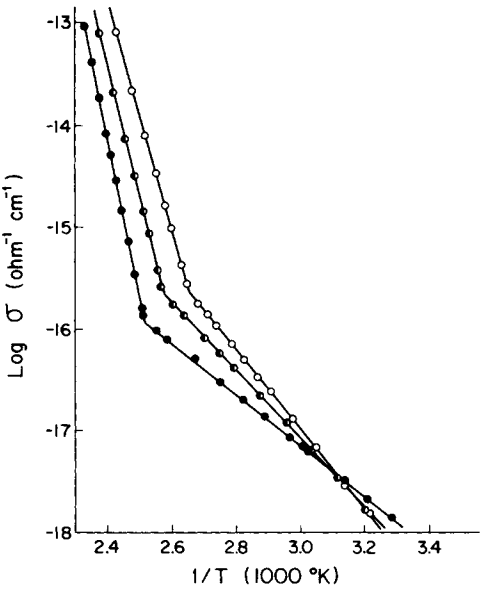


Fig. 10. Electrical conductivity ($\sigma$) vs. reciprocal temperature for epoxide resins: (○) sample 1; (◐) sample 2; (●) sample 3.

## DISCUSSION

Epoxide resins have complicated structures, and various characteristics can be obtained by controlling the curing conditions. In this investigation, epoxide resins cured as completely as possible and having various ratios of ester and ether bonds have been studied. The introduction of an ester link to the cured epoxide resin networks increases its $T_g$. This behavior is caused by the bulky phenyl group chain of methyltetrahydrophthalic acid anhydride curing agent which reacts with the epoxy group to form the ester link. It restricts the molecular mobility owing to steric hindrance, yielding a high $T_g$. It is known that the glass transition phenomena influence electric properties as well as physical, chemical, and mechanical properties. In this temperature region, for instance, dielectric properties,[10,11] thermostimulated current properties,[12,13] thermoluminescent properties,[14] and photoconduction properties[15] are changed abruptly. It has also been pointed out that the charge transportation and the conditions of carrier trap are related to the molecular motion of main chains of polymers.

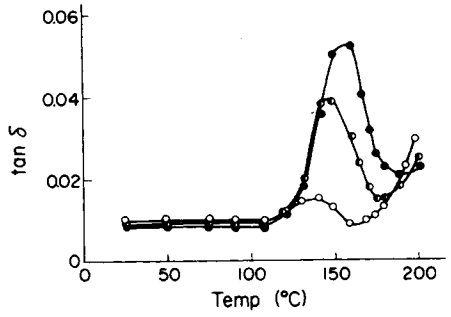


Fig. 11. Dielectric loss tangent (tan $\delta$) vs. temperature for epoxide resins at 60 Hz: (○) sample 1; (◐) sample 2; (●) sample 3.

The outstanding feature of the results presented is that critical temperatures obtained from electric strength measurement seem to be strongly related to $T_g$, at which the diffusional motion of the polymer increases. It is to be inferred, therefore, that there is a considerable importance in the free volume and the molecular relaxation process of the polymers in determining the change in electric strength. Table III shows a comparison of the transition temperatures which were deduced from specific volume, electrical conductivity, and electric strength. Here, $T_g$ and $T_c$ are the intersection temperatures of the oblique lines detected by temperature dependence of specific volume and electrical conductivity, respectively. $T_b$ is the critical temperature at which a marked reduction in the electric strength occurs. Precise determination of $T_b$ is not easy because of the scattering of points of strength. Therefore, the temperature is indicated by the range. Fairly good agreement is observed between $T_g$ and $T_c$. The $T_b$ temperature region is also the same as that of $T_g$ and $T_c$, although some less pronounced temperature differences appear in each of the samples. Taking the difficulty in measuring $T_b$ into consideration, these three values coincide well, and it is apparent that molecular motions, electrical conductivity, and electric breakdown behavior relate significantly. $T_g$ can usually be identified at the onset of diffusional motion of the main chain of the polymer. With increasing temperature, a segmental motion occurs, and the greater mobility of the polymer segments results at the same time in an increase in the free volume of the polymer. This behavior is reflected in the curvature of the temperature dependence of conductivity plots. Therefore, marked increase in conductivity at temperature above $T_g$ is considered to favor the ionic conduction mechanism in these polymers.[16,17]

At high electric fields, the current density $J$ for ion transportation in general follows the sin h theory in eq. (2)[18]:

$$J = en\nu\lambda \exp(eF\lambda/2kT) \exp(-E/KT) \qquad q\lambda F \ll 2kT \tag{2}$$

where $e$ is the charge, $n$ the density of the electric charge, $F$ the electric field, $E$ the activation energy, $k$ Boltzmann's constant, $T$ the absolute temperature, $\lambda$ the jump distance of the ion, and $\nu$ the frequency of vibrations of the

$$\log J = (e\lambda/2kT)F + \log J_0 \tag{3}$$

where $en\nu\lambda \exp(-E/kT) = J_0$.

Figure 12 shows the behavior of the current over a wide range of electric field for each sample. The observed linearity in the log $J$ vs. $F$ plots at high electric field following eq. (3) is considered to justify the idea of ion transportation; this means that an ionic charge carrier is also important in this precursory region of electric breakdown. Artbauer[19,20] has indicated that the polymer would fail electrically when the energies acquired by accelerated electrons increase to a

TABLE III
Comparison of $T_g$, $T_c$, and $T_b$ of epoxide resins.

| Sample No. | $T_g$ (°C) | $T_c$ (°C) | $T_b$ (°C) |
|---|---|---|---|
| 1 | 108 | 103 | 100 ~ 110 |
| 2 | 115 | 114 | 105 ~ 115 |
| 3 | 125 | 125 | 110 ~ 120 |

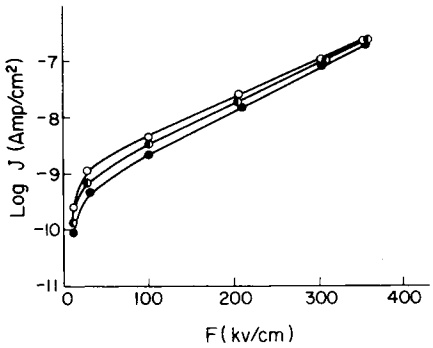


Fig. 12. Current density ($J$) vs. electric field ($F$) of epoxide resins at 150°C: (○) sample 1; (◐) sample 2; (●) sample 3.

critical value after transit through voids such as free volume present in the polymer; therefore the extent of the free volume exhibited by the structure assumes considerable importance. But it is also likely that the ion transfer process through voids play an important part to increase the energies in the precursory region of electric breakdown. This explanation concerning free volume is adequate to explain the abrupt change of electric strength at $T_g$. It is, however, insufficient to explain the present results above $T_g$.

The pulse breakdown behavior above $T_g$ shows the pulse width dependence and a longer time of applied voltage results in a lower electric strength. Direct current breakdown behavior at 150°C shows a dependence on sample film thickness. Such behavior means that the amount of energy applied to epoxide resins and the heat discharge from them are very important for electric breakdown. Thermal equilibrium for charge and discharge energy in general is given by[21]

$$Cv(dT/dt) - \text{div}(K \text{ grad } T) = \delta F^2 \tag{4}$$

where $Cv$ is the heat capacity, $dT/dt$ the temperature change per unit time, $K$ the thermal conductivity, $T$ the absolute temperature, $\delta$ the electrical conductivity, and $F$ the electric field. The results shown in this investigation at high temperatures support the thermal breakdown mechanism which is based on eq. (4). If the temperature is high enough, the sample film may be unable to dissipate the heat from the region where it is generated, and breakdown must occur. The electric strength is also affected by the structural differences of epoxide resin networks in this region above $T_g$, and introduction of ester links causes the electric strength to decrease. Such behavior should be considered with the polymer relaxation process and can be related to the absorption current as the absorption current is usually composed of a relaxation process of dipole orientation. In Figure 11, the tan $\delta$ peak which is assigned to the $\alpha$-relaxation of epoxide resins is based on orientation of polar segments. It is therefore found that the energy loss of polymers in this region becomes serious. Such energy loss will increase with rising electric field and generate considerable heat. The presence of an ester link in the polymer network has the effect of a reduction in electric strength under equal conditions at a characteristically higher temperature region. This behavior explains the fact that the resultant dipole moment, caused by introducing the ester bond in epoxide resins, increases the magnitude of peak

loss. Therefore, the temperature rise of the film will be accelerated and consequently the strength will decrease.

## CONCLUSIONS

Epoxide resins having various ratios of ether and ester bonds were investigated. The breakdown behavior and underlying mechanism at relatively high temperatures were discussed.

Very significant relations between polymer nature and electric breakdown behavior and good coincidence of $T_g$, $T_c$, and $T_d$ were observed. Above $T_g$, ions apparently play an important part of conduction in the precursory region of electric breakdown in epoxide resins. In this temperature region, the electric strength has a strong dependence on polymer structures, film thickness, and applied pulse width. Although the difficulties in the derivation of quantitative relations prevent further mathematical treatment, the tendencies above $T_g$ are consistent with those of a thermal breakdown mechanism.

## References

1. M. W. Ranney, *Epoxy Resins and Products, Recent Advances*, New Jersey, 1977.
2. K. Dusek, J. Plestil, F. Lednicky, and S. Lunak, *Polymer*, **19,** 393 (1978).
3. O. Milton, *Insulation*, 59 (November 1967).
4. R. E. Cuthrell, *J. Appl. Polym. Sci.*, **12,** 955 (1968).
5. R. E. Cuthrell, *J. Appl. Polym. Sci.*, **12,** 1263 (1968).
6. R. E. Cuthrell, *J. Appl. Polym. Sci.*, **16,** 1983 (1972).
7. A. V. Tobolsky, *Properties and Structure of Polymers*, Wiley, New York, 1960.
8. D. Katz and A. V. Tobolsky, *Polymer*, **4,** 417 (1963).
9. T. L. Smith, *J. Polym. Symp.*, **46,** 97 (1974).
10. J. G. Kirkwood, *J. Chem. Phys.*, **14,** 51 (1946).
11. O. Nakada, *J. Phys. Soc. Jpn.*, **10,** 804 (1955).
12. J. T. Randall and M. H. F. Wilkinson, *Proc. Roy. Soc. Ser. A*, **184,** 366 (1945).
13. S. Unger and M. M. Perlman, *Phys. Rev.*, **B6**(10), 3973 (1972).
14. A. Charlesby and R. H. Partridge, *Proc. Roy. Soc. Ser. A*, **271,** 170 (1963).
15. T. Tanaka and Y. Inuishi, *J. Appl. Phys.*, **5,** 974 (1966).
16. T. Miyamoto and K. Shibayama, *Kobunshi Kagaku*, **30** (334), 103 (1973).
17. S. Saito, *Rep. Progr. Polym. Phys. Japan*, **12,** 411 (1969).
18. M. Kosaki, K. Sugiyama, and M. Ieda, *J. Appl. Phys.*, **42** (9), 3388 (1971).
19. J. Artbauer, *ACTA Tech. CSAV*, **No. 3,** 416 (1966).
20. J. Artbauer, *ACTA Tech. CSAV*, **No. 3,** 429 (1966).
21. S. Whitehead, *Dielectric Breakdown of Solids*, Clarendon, Oxford, 1951.

Received July 30, 1979
Accepted July 7, 1980
Corrected proofs received April 27, 1981